CHEMISTRY
A EUROPEAN JOURNAL

DOI: 10.1002/chem.200500410

Mono- and Dinuclear Bioxazoline–Palladium Complexes for the Stereocontrolled Synthesis of CO/Styrene Polyketones

Alessandro Scarel,[a] Jérôme Durand,[a] Davide Franchi,[a] Ennio Zangrando,[a] Giovanni Mestroni,[a] Carla Carfagna,[b] Luca Mosca,[b] Roberta Seraglia,[c] Giambattista Consiglio,[d] and Barbara Milani*[a]

Abstract: The coordination chemistry of the chiral bioxazoline ligand (4*S*,4′*S*)-2,2′-bis(4-isopropyl-4,5-dihydrooxazole) to Pd^{II} provides evidence that the ligand bonding can occur either through chelation of one Pd^{II} ion leading to a mononuclear species with the expected *cis* geometry, or by double bridging of two Pd^{II} ions giving a dinuclear complex with *trans* geometry. The species in solution are identified by ^1H NMR spectroscopy. Both the mononuclear and the dinuclear complexes promote the CO/styrene copolymerization, yielding the corresponding polyketone with a fully or a predominantly isotactic microstructure, depending on the reaction medium. The nature of the anion present in the palladium precatalysts affects the polyketone stereochemistry. MALDI-TOF analysis of the copolymers synthesized reveals the presence of *p*-hydroxyphenolic end-groups, thus confirming and explaining the role of 1,4-hydroquinone as a molecular weight regulator.

Keywords: copolymerization · mass spectrometry · N ligands · palladium · polyketones

Introduction

Development of new polymeric materials is considered one of the major goals of contemporary chemistry and homogeneous catalysis constitutes a powerful tool to reach this target by achieving, at the same time, fine tuning of the structural features of macromolecules synthesized, with particular attention to control of their stereochemistry.[1]

Asymmetric polymerization represents a very important class of enantioselective reactions. It includes three major categories: 1) asymmetric synthesis polymerization; 2) helix-sense-selective polymerization; 3) enantiomer-discriminating polymerization.[2] In the first category, a prochiral monomer is polymerized to give a polymer with main-chain chirality. Only a few examples of such polymers are known; among them are the isotactic CO/α-olefin polyketones.[3]

Polyketones can be divided into two main classes based on the olefin comonomer: CO/aliphatic and CO/aromatic olefin copolymers. The nature of the olefin dictates which ancillary ligand is preferred for the catalytic system which promotes the copolymerization reaction. For instance, nitrogen donors are the ligands of choice for the copolymerization of CO with aromatic olefins. In this respect, the first synthesis of the isotactic CO/*p*-*t*Bu-styrene (*p*-*t*Bu-styrene = *p*-*tert*-butylstyrene) copolymer was reported by Brookhart and co-workers in 1994, promoted by a palladium complex modified with the enantiomerically pure C_2-symmetric bisoxazoline (2,2-bis{2-[(4*S*)-4-methyl-1,3-oxazolinyl]}propane).[4] This reaction is a rare example of asymmetric, perfectly alternating, *living* copolymerization. One year later, Carfagna and co-workers reported the synthesis of the isotactic CO/styrene and CO/*p*-Me-styrene (*p*-Me-styrene = *p*-methylstyrene) copolymers based on the use of a palladium complex with the enantiomerically pure C_2-symmetric bioxa-

[a] A. Scarel, Dr. J. Durand, D. Franchi, Prof. E. Zangrando, Prof. G. Mestroni, Dr. B. Milani
Dipartimento di Scienze Chimiche,Università di Trieste
Via Licio Giorgieri 1, 34127 Trieste (Italy)
Fax: (+39) 040-558-3903
E-mail: milani@dsch.units.it

[b] Dr. C. Carfagna, Dr. L. Mosca
Istituto di Scienze Chimiche, Università di Urbino
Piazza Rinascimento 6, 61029 Urbino (Italy)

[c] Dr. R. Seraglia
CNR, Istituto di Scienze e Tecnologie Molecolari Sez. di Padova
Via Marzolo 1, 35020 Padova (Italy)

[d] Prof. G. Consiglio
Eidgenössische Technische Hochschule
Institut für Chemie- und Bioingenieurwissenschaften
ETH-Hönggerberg
8093 Zürich (Switzerland)

zoline (4*S*,4′*S*)-2,2′-bis(4-isopropyl-4,5-dihydrooxazole) ((*S*,*S*)-*i*Pr-BIOX).[5] Since then, a wide variety of chiral nitrogen-donor chelating ligands (N*–N*) of different symmetry was applied to this reaction,[6] together with the phosphino-phosphito derivative BINAPHOS[7] and several hybrid P–N ligands.[8] All the systems based on N*–N* ligands suffer from rather poor stability of the active species, which prevents the synthesis of the isotactic polyketones in high yields and with high molecular weights. The catalytic system based on P–N ligands is the uniquely able to promote the synthesis of the isotactic CO/styrene copolymer, reaching productivities of up to 18 g CP (g Pd)$^{-1}$ h^{-1} (CP = copolymer), but it requires quite drastic reaction conditions, such as a CO pressure of 320 bar.[8b] Dichloromethane, chlorobenzene, or methanol are the preferred solvents for this reaction.

Our research in this field has addressed the synthesis of syndiotactic CO/aromatic olefin copolymers promoted by Pd^{II} bischelated derivatives $[Pd(N–N)_2][PF_6]_2$ (N–N = 1,10-phenanthroline (phen), 2,2′-bipyridine (bpy), and their substituted derivatives). This copolymerization succeeds when it is carried out in a fluorinated alcohol, such as 2,2,2-trifluoroethanol (TFE), which remarkably contributes to the stability of the active species, allowing synthesis of the corresponding polyketones with yields up to 17 kg CP (g Pd)$^{-1}$ (362 g CP (g Pd)$^{-1}$ h^{-1})[9a,b] and molecular weights around 300 000.[9c,d] These values are much higher than those obtained for the reaction in methanol, the solvent of choice in the literature catalytic systems. Very recently, we demonstrated the positive effect of trifluoroethanol even when monochelated complexes [Pd(Me)(MeCN)(N–N)][X] (X = OTf (OTf = triflate), PF_6^-) were used as precatalysts.[10]

We have now approached the problem of the stability of the active species even in the synthesis of the isotactic copolymer, taking into account the catalytic system based on the bioxazoline ligand (*S*,*S*)-*i*Pr-BIOX. Although chiral bioxazoline ligands are among the most successful, versatile, and commonly used classes of ligands for asymmetric catalysis,[11] their coordination chemistry to palladium has not yet been investigated deeply.

We report herein a detailed investigation of the coordination chemistry of this ligand to palladium, together with the catalytic behavior of complexes [Pd(Me)(MeCN)((*S*,*S*)-*i*Pr-BIOX)][X] (X = OTf **1**, PF_6 **2**, BArF **3** (BArF = B[3,5-$(CF_3)_2C_6H_3]_4^-$)) in the CO/styrene copolymerization reaction. New insights into the mechanism of this reaction are highlighted by MALDI-TOF analysis of polyketone end-groups.

Results and Discussion

Synthesis and characterization of palladium complexes 1–3 and of their precursor [Pd(Me)(Cl)((*S*,*S*)-*i*Pr-BIOX)] 4: The palladium complexes [Pd(Me)(MeCN)((*S*,*S*)-*i*Pr-BIOX)][X] **1–3** were synthesized in a five-step procedure from $[Pd(OAc)_2]$,[10,12] which implies the isolation of the neutral derivative [Pd(Me)(Cl)((*S*,*S*)-*i*Pr-BIOX)] (**4**).

Complex **4** was characterized both in the solid state and in solution. Two kinds of single crystals were isolated, depending on the conditions for crystal growth. The single crystals obtained directly from the synthetic mixture correspond to the mononuclear species **4** (Figure 1a). Recrystallization of **4** in a dichloromethane/hexane mixture yielded, together with the yellow crystals of **4**, orange crystals which correspond to the dinuclear species [{Pd(Me)(Cl)(μ-(*S*,*S*)-*i*Pr-BIOX)}$_2$] (**4a**) (Figure 1b).

In the mononuclear complex **4** the palladium atom displays the expected square-planar coordination geometry with Pd–N1 and Pd–N2 bond lengths significantly different (2.059(4) and 2.189(4) Å, respectively); the longer bond reflects the *trans* influence exerted by the methyl group (Table 1). The Pd–C(methyl) and Pd–Cl bond lengths

Table 1. Selected bond lengths [Å] and angles [°] for **4**.

Pd–C1	2.017(4)	C1-Pd-N2	171.6(2)
Pd–N1	2.059(4)	N1-Pd-N2	77.88(15)
Pd–N2	2.189(3)	C1-Pd-Cl1	91.50(16)
Pd–Cl1	2.3021(15)	N1-Pd-Cl1	174.67(11)
C1-Pd-N1	93.8(2)	N2-Pd-Cl1	96.79(11)

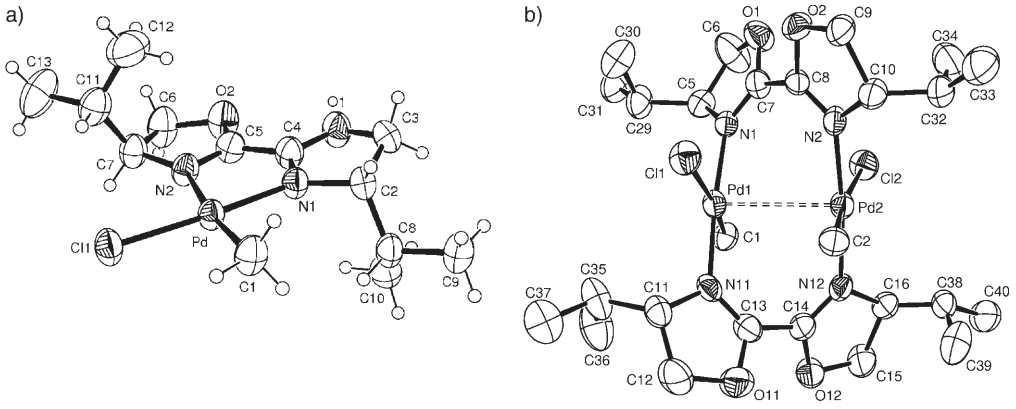

Figure 1. ORTEP drawing (thermal ellipsoids at 40% level) with the atom labeling scheme of **4** and of one of the two crystallographically independent molecules of **4a**.

(2.017(4) and 2.3021(15) Å, respectively) compare well with distances found in analogous complexes.[6c,13] The chelating N1-Pd-N2 bond angle is 77.88(15)°; the oxazoline planes are almost coplanar, and the tilting angle between the mean planes is 9.0(2)°. X-ray analysis of complex **4a** (Figure 1b) shows two crystallographically independent molecules of closely comparable conformation in the unit cell. The palladium atoms are doubly bridged by bioxazoline ligands and complete the distorted square-planar coordination sphere through a methyl group and a chloride in *trans* positions to each other. The coordination bond lengths in the two molecules show a considerable variation (Table 2): Pd–N varies from 2.009(8) to 2.045(7) Å and Pd–C from 2.030(9) to 2.099(8) Å, while Pd–Cl falls within a narrower range. Among the coordination bond angles, C-Pd-Cl, which averages 172°, manifests the largest distortion from the ideal square-planar geometry.

Table 2. Selected bond lengths [Å] and angles [°] for **4a**·0.5 CH_2Cl_2.

	Molecule A		
Pd1–N11	2.036(8)	Pd2–N2	2.036(7)
Pd1–N1	2.045(7)	Pd2–N12	2.037(7)
Pd1–C1	2.099(8)	Pd2–C2	2.075(9)
Pd1–Cl1	2.449(2)	Pd2–Cl2	2.453(2)
Pd1–Pd2	2.9575(12)		
N11-Pd1-N1	175.2(3)	N2-Pd2-N12	174.5(3)
N11-Pd1-C1	89.4(3)	N2-Pd2-C2	89.4(3)
N1-Pd1-C1	89.6(3)	N12-Pd2-C2	88.9(3)
N11-Pd1-Cl1	92.6(2)	N2-Pd2-Cl2	89.4(2)
N1-Pd1-Cl1	88.93(19)	N12-Pd2-Cl2	93.0(2)
C1-Pd1-Cl1	172.0(3)	C2-Pd2-Cl2	172.2(3)
N1-Pd1-Pd2-N2	45.3(3)	N11-Pd1-Pd2-N12	42.2(3)
	Molecule B		
Pd3–N13	2.009(8)	Pd4–N14	2.033(8)
Pd3–N3	2.013(8)	Pd4–N4	2.037(7)
Pd3–C3	2.030(9)	Pd4–C4	2.069(9)
Pd3–Cl3	2.461(2)	Pd4–Cl4	2.460(2)
Pd3–Pd4	2.9582(15)		
N13-Pd3-N3	175.7(3)	N14-Pd4-N4	174.2(3)
N13-Pd3-C3	87.9(4)	N14-Pd4-C4	88.1(3)
N3-Pd3-C3	89.5(4)	N4-Pd4-C4	89.7(3)
N13-Pd3-Cl3	91.1(2)	N14-Pd4-Cl4	89.6(2)
N3-Pd3-Cl3	91.9(2)	N4-Pd4-Cl4	93.3(2)
C3-Pd3-Cl3	173.1(3)	C4-Pd4-Cl4	171.8(3)
N3-Pd3-Pd4-N4	40.7(3)	N13-Pd3-Pd4-N14	45.6(3)

The ^{1}H NMR spectra of **4** and **4a** in solution also indicate the complex nuclearity (Figure 2). In the ^{1}H NMR spectrum of **4** the number of bioxazoline ligand signals is in agreement with its coordination in a nonsymmetrical chemical environment.[5b] The Pd–CH_3 fragment gives a singlet at δ = 1.02 ppm, while the multiplet between δ = 0.84 and 0.99 ppm is assigned to the methyl groups of the isopropyl substituents. The corresponding CH groups give two multiplets centered at δ = 2.26 and 2.74 ppm (Figure 2a). The two multiplets centered at δ = 4.37 and 4.26 ppm are assigned to H^4 and $H^{4'}$, while the signals between δ = 4.53 and 4.74 ppm are due to protons in position 5. The NOE observed upon irradiation of the Pd–CH_3 signal made it possible to assign the multiplet at δ = 2.74 ppm, and consequently those at δ = 4.37 and at 4.53 ppm (correlated in the HH COSY spectrum), to the protons of the heterocyclic ring *cis* to the Pd–CH_3 group.

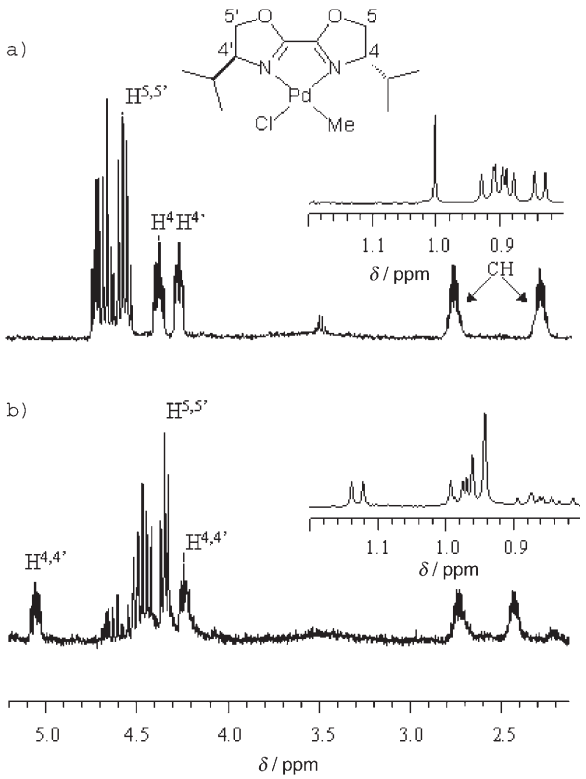

Figure 2. ^{1}H NMR spectra in $CDCl_3$ at room temperature of complexes: a) **4**; b) **4a**. Inset: the region of the methyl signals.

In the spectrum of **4a** the Pd–CH_3 singlet is at δ = 0.94 ppm, the frequencies attributed to the methyl groups of the isopropyl substituents are in the frequency range $0.84 \leq \delta \leq 1.19$ and the corresponding CH generate two multiplets centered at δ = 2.48 and 2.78 ppm, respectively (Figure 2b). The other two multiplets centered at δ = 4.29 and 5.10 ppm are assigned to protons in positions 4 and 4′. The number of signals and their integration are in agreement with the symmetry of the dinuclear species, which makes the two halves of each bioxazoline ligand equivalent (the C_2 symmetry axis passes through the C–C bond that links the two dihydroxazoline rings), but not the two molecules of the facing bioxazolines (there is no C_2 symmetry axis along the Pd–Pd internuclear axis).

Thus, by comparison of the two spectra some signals can be recognized as characteristic of mononuclear and dinuclear complexes. In particular, in the spectrum of the dinuclear derivative (Figure 2b), one of the two multiplets of H^4 is shifted to higher frequency with respect to the same signals in the mononuclear derivative (Figure 2a) and it appears downfield even from the multiplets attributed to $H^{5,5'}$. An analogous shift, even if less pronounced, is observed for one of the two multiplets assigned to the CH of the isopropyl substituents; also, a different pattern is shown by the methyl group signals of these substituents, which are spread

over a wider frequency range than the corresponding signals in the mononuclear derivative.

The neutral species **4** is transformed into the monocationic species **1–3** by treatment with the appropriate silver salt, AgX, or NaBArF, in the presence of acetonitrile. Single crystals of the triflate derivative **1** are obtained directly from the reaction mixture. The X-ray diffraction analysis (Figure 3) reveals that the compound has a structure analogous to that of **4a**, with the bioxazoline ligands bridging two palladium ions and the triflates replacing the chlorides. Thus, it must be better formulated as [{Pd(Me)(OTf)(μ-(*S,S*)-*i*Pr-BIOX)}$_2$] (**1a**). The palladium atoms, separated by 2.8938(8) Å (Table 3), are slightly closer than in **4a**. The square-planar environments are rather distorted and, as observed in **4a**, the most relevant deviations are exhibited by the *trans* O-Pd-C bond angles of about 171°. In both **4a** and **1a**, the two square-planar coordination planes are parallel and staggered with N-Pd1-Pd2-N torsion angles that average 44° and 42°, respectively. Apparently, the replacement of chloride with the bulkier triflate does not cause any modification in the overall geometry, thus suggesting that steric interactions are not responsible for the differences in the Pd–Pd distances.

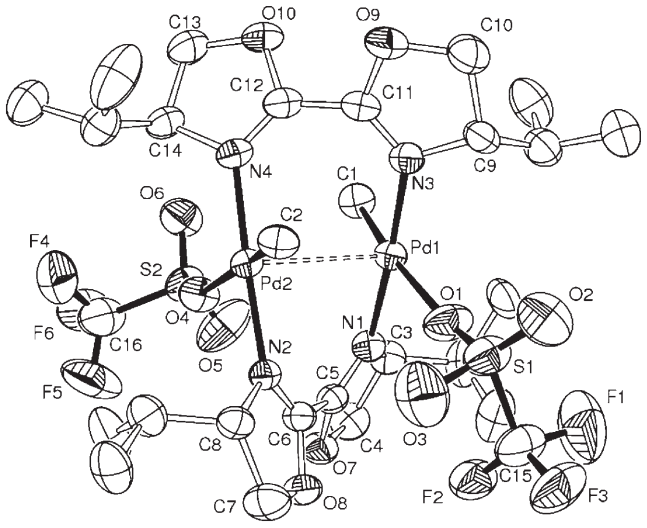

Figure 3. ORTEP drawing (thermal ellipsoids at 35% level) with the atom labeling scheme of complex **1a**.

Table 3. Selected bond lengths [Å] and angles [°] for **1a**.

Pd1–C1	1.996(7)	Pd2–C2	2.000(7)
Pd1–N3	2.038(6)	Pd2–N4	2.027(5)
Pd1–N1	2.055(5)	Pd2–N2	2.036(5)
Pd1–O1	2.218(6)	Pd2–O4	2.273(5)
Pd1–Pd2	2.8938(8)		
C1-Pd1-N3	88.4(3)	C2-Pd2-N4	89.5(3)
C1-Pd1-N1	89.7(3)	C2-Pd2-N2	90.2(2)
N3-Pd1-N1	176.5(2)	N4-Pd2-N2	177.2(2)
C1-Pd1-O1	170.9(4)	C2-Pd2-O4	170.7(3)
N3-Pd1-O1	93.3(2)	N4-Pd2-O4	94.5(2)
N1-Pd1-O1	89.1(2)	N2-Pd2-O4	86.2(2)
N3-Pd1-Pd2-N4	40.7(2)	N1-Pd1-Pd2-N2	43.4(2)

A few examples of other bioxazoline ligands bridging metal ions have been reported.[14–16] Thus, the present dinuclear complexes with bridging bioxazoline characterize unprecedented structures; therefore their structural features deserve a more detailed discussion. In both complexes the metal–metal distance of about 2.90 Å does not exclude an interaction between the palladium atoms, since each metal ion is displaced slightly inward from its coordination mean plane, that is, toward the other metal center (mean displacement = 0.04 Å). The two complexes **4a** and **1a** possess virtual twofold symmetry (although no crystallographic rotational symmetry is present) with the axis passing through the central oxazoline C–C bonds. The *trans* bioxazoline ligands induce the Pd square-planar planes to be facing each other, but with a configuration staggered by means of a significant propeller tilt of the bioxazoline. The latter aspect represents the key element defining the helical arrangement in these complexes. In theory, with optically pure (*S,S*)-bioxazoline, two diastereoisomers can be formed, but both **1a** and **4a** display a *P* handedness. The preferential formation of only one diastereoisomer, when optically pure ligands are used, is widely documented in various helicate coordination compounds.[14,17]

The ^{1}H NMR spectra of complexes **1a, 2** and **3** in solution differ, depending on the nature of the anion (Figure 4). In particular, the spectrum of **1a** is analogous to that of **4a** with one of the two signals attributed to $H^{4,4'}$ at high frequency, confirming the dinuclear nature of the complex, even in solution. By taking advantage of the new knowledge about the characterization in solution of these complexes, it is possible to identify complex **3** as the mononuclear species [Pd(Me)(MeCN)((*S,S*)-*i*Pr-BIOX)][BArF] and complex **2** as the 2:1 mixture of the dinuclear and mononuclear species, with one molecule of acetonitrile occupying the fourth position of the palladium coordination sphere in the dinuclear complex. The difference between these complexes was also confirmed by ESI spectra (see Experimental Section).

CO/styrene copolymerization: Complexes **1a, 2**, and **3** were tested as catalysts for the CO/styrene copolymerization under reaction conditions similar to those reported in the literature:[4a,5a,10] 1 atm CO pressure, in the presence of 1,4-benzoquinone for 4 h. A glass reactor was used so that the evolution of the system could be monitored visually.

When dichloromethane was the reaction medium, only traces of polyketone were obtained because of fast decomposition of the active species to inactive palladium metal (Table 4). Among the complexes studied, the catalyst with BArF showed the highest catalytic activity with a productivity of 11 g CP(g Pd)$^{-1}$ h^{-1}.

The change of solvent from dichloromethane to 2,2,2-trifluoroethanol resulted in a remarkable increase in the productivity; an increase of one order of magnitude was achieved when complex **3** was used (productivity 101 g CP-

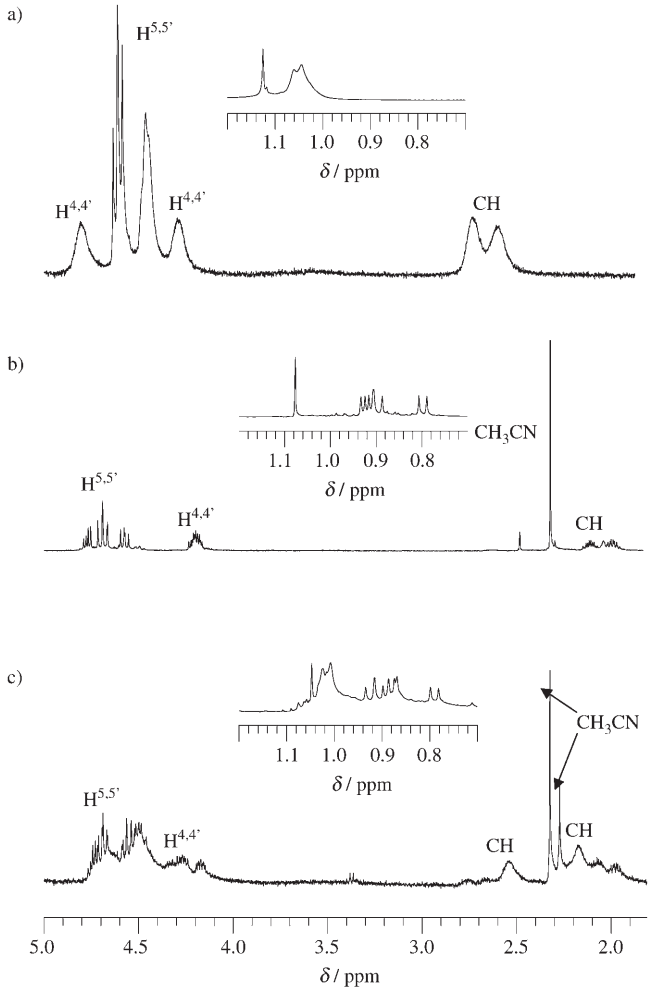

Figure 4. ^{1}H NMR spectra in CD_2Cl_2, at room temperature of complexes: a) **1a**; b) **3**; c) **2**. Inset: the region of the methyl signals.

Table 4. CO/styrene copolymerization: effect of solvent and anion (catalyst precursor: **1a**, **2** and **3**).[a]

X	Solvent	[g CP]	[g CP(g Pd)$^{-1}$]h^{-1}	$\langle M_w\rangle$ ($\langle M_w\rangle/\langle M_n\rangle$)
BArF **3**	CH_2Cl_2	0.06	11	n.d.
PF_6 **2**	CH_2Cl_2	traces	n.d.	n.d.
OTf **1a**	CH_2Cl_2	traces	n.d.	n.d.
BArF **3**	TFE	0.55	101	3300 (1.4)
PF_6 **2**	TFE	0.31	57	3900 (1.3)
OTf **1a**	TFE	0.33	61	3500 (1.4)

[a] Reaction conditions: $n_{Pd} = 1.27\times10^{-5}$ mol; $n_{BQ} = 5.1\times10^{-4}$ mol; styrene $V = 10$ mL; solvent $V = 20$ mL; $T = 30$ °C; $P_{CO} = 1$ atm; $t = 4$ h; [BQ]/[Pd] = 40. n.d. = not determined.

(Pd)$^{-1}$h^{-1}) (Table 4). The molecular weights of the synthesized copolymers were still quite low (<4000) (Table 4).

The effect of the anion on productivity is now clearly evident: similar values are obtained when complexes with PF_6 and OTf are tested, while the BArF derivative **3** remains the most active among the three (Table 4). The highest productivity shown by this complex is in agreement with the results of a previous investigation on the effect of the anion on the activity of complexes [Pd(η^1,η^2-C_8H_{12}OMe)(bpy)][X] as precatalysts for this reaction.[18] To understand whether the effect of the anion on the productivity might be related to the difference in nature of the corresponding precatalysts, the reactivity of complexes **1a** and **2** with CO was investigated by in situ NMR experiments both in neat CD_2Cl_2 and in a CD_2Cl_2/CF_3CH_2OH mixture (the reactivity of **3** with CO and *p*-methylstyrene has been studied recently).[5b] When a CD_2Cl_2 solution of **2** is treated with carbon monoxide, the mononuclear complex is transformed into the Pd–acyl species, while the dinuclear derivative appears to be inert toward carbonylation. This behavior is reasonable, because the dinuclear species does not possess the required geometry for an insertion reaction, as the Pd−Me group and the acetonitrile are in *trans* positions. However, when **2** reacts with carbon monoxide in CD_2Cl_2 solution (0.7 mL) containing 2.7 μL trifluoroethanol (TFE), the Pd–acyl species is formed almost quantitatively, suggesting that the fluorinated alcohol favors the transformation of the dinuclear complex to a species suitable to undergo CO insertion, probably a mononuclear complex. When the same experiments are performed on complex **1a**, even in the presence of 2.7 μL TFE, only a very small amount of the Pd–acyl species is formed, thus indicating that, in this case, the reaction with CO is not as easy as for complex **2**. On the basis of these results, it appears that the very low catalytic activity of complexes **1a** and **2** (in comparison with **3**) in dichloromethane might be due initially to the difficulty in forming the first Pd–acyl species. However, even after the polymerization has started, the stability of the active species is very low, yielding only traces of copolymer regardless to the nature of the anion.

No decomposition of the active species to palladium metal was observed when the copolymerizations took place in the fluorinated solvent. Therefore, the main effect of the fluorinated alcohol is to enhance the stability of the catalyst remarkably, as we already reported when TFE was used either in place of methanol in the catalytic system based on the bischelated complexes [Pd(N–N)$_2$][PF_6]$_2$,[9b] or in place of dichloromethane in the system based on monochelated complexes [Pd(Me)(MeCN)(N–N)][X].[10] The positive effect of TFE on the catalytic system based on bioxazoline ligands is not trivial. Indeed, when the fluorinated alcohol was used in place of dichloromethane, with pyridine–oxazoline–palladium complexes, because of the fast and complete decomposition of catalyst to palladium metal no catalytic activity was observed.[19] It is logical that, with the present complexes, the trifluoroethanol is required to favor the transformation of the inert dinuclear species into a reactive intermediate.

Both when the benzoquinone/palladium ratio was increased (Table 5, runs 1–3) as well as when the reaction time was prolonged (Table 5, runs 3–6) a modest increase in the productivity was found, associated with a clear decrease in the molecular weights.

Table 5. CO/Styrene copolymerization: effect of benzoquinone concentration and of reaction time (catalyst precursor: **2**).[a]

Run	Time [h]	[BQ]/[Pd]	[g CP]	[g CP (g Pd)$^{-1}$]	$\langle M_w \rangle$ ($\langle M_w \rangle / \langle M_n \rangle$)
1	4	10	0.09	66	4800 (1.3)
2	4	20	0.16	120	4500 (1.3)
3	4	40	0.31	228	3900 (1.3)
4	8	40	0.45	330	4200 (1.3)
5	16	40	0.83	630	3900 (1.4)
6	24	40	1.02	750	3000 (1.3)

[a] Reaction conditions: $n_{Pd} = 1.27 \times 10^{-5}$ mol; solvent TFE $V = 20$ mL; styrene $V = 10$ mL; $T = 30\,°C$; $P_{CO} = 1$ atm.

Characterization of polyketones: The stereochemistry of the polyketones was studied by ^{13}C NMR spectroscopy by recording the spectra in a mixture of 1,1,1,3,3,3-hexafluoroisopropanol (HFIP) and $CDCl_3$. The microtacticity was determined by integration of the signals due to the *ipso*-carbon atom (Table 6). In agreement with the literature data,[5] the

Table 6. Percentage triad distribution in CO/styrene polyketones (catalyst precursor: **1a**, **2**, and **3**).[a]

X	Solvent	*ll*	*ul*	*lu*	*uu*	$[\alpha]_D^{25}$[b]
BArF **3**	CH_2Cl_2	>99	0	0	0	−346
PF_6 **2**	CH_2Cl_2	>99	0	0	0	n.d.
OTf **1a**	CH_2Cl_2	>99	0	0	0	n.d.
BArF **3**	TFE	76	8	8	8	−265
PF_6 **2**	TFE	73	9	9	9	−267
OTf **1a**	TFE	61	14	14	10	−238

[a] ^{13}C NMR spectra recorded in HFIP (0.9 mL) plus $CDCl_3$ (0.4 mL) at room temperature. [b] Optical activity measured in $CHCl_3$, $c = 0.1$ g-(100 mL)$^{-1}$.

polyketones prepared in dichloromethane are completely isotactic, only the *ll* triad being visible and the optical activity being in the expected range. In the ^{13}C NMR spectra of the polyketones synthesized in TFE the signals of all the four triads are present with different intensities. The major signal is always associated with the *ll* triad, so the polyketones produced still have a prevailingly isotactic microstructure, even if the stereoregularity is lower than that of the polyketones synthesized in CH_2Cl_2 (Table 6). Moreover, the anion effect on the tacticity of the polyketones is now evident. A very similar triad distribution is observed in the spectra of polyketones synthesized with precatalysts **2** and **3**, while the copolymer prepared with precatalyst **1a** has the lowest content of the *ll* triad. The optical activity values are in agreement with the microtacticity determined by the ^{13}C NMR spectra.

From the results reported here and in the very recent literature,[20,21,22] it is clear that the control of the stereochemistry in the CO/styrene copolymerization reaction is not only related to the symmetry of the N–N ligand present in the palladium coordination sphere, but it is affected by other factors, such as the reaction medium, the anion, the nature of the precatalyst, and the ligand/palladium ratio. While the effect of these parameters, in particular of the role played by the anion, on the polymer stereochemistry has been being investigated for several years in the synthesis of polypropene,[23] in the case of CO/olefin copolymerization the study of this aspect is at an early stage, the first report having appeared in 2002.[20] It has been reported that [Pd(*m*-Bz-BIOX)$(H_2O)_2$][OTf]$_2$ (*m*-Bz-BIOX = (4*R*,4′*S*)-2,2′-bis(4-benzyl-4,5-dihydrooxazole)) leads to the isotactic polyketone when the copolymerization is carried out in CH_2Cl_2/MeOH (9:1), while the syndiotactic copolymer is the product when pure MeOH is the solvent.[20] Moreover, the same complex promotes the synthesis of syndiotactic polyketones in CH_2Cl_2/MeOH (9:1) when the counterion is BF_4^- or PF_6^- instead of triflate.[21] The effect of the anion is also shown in the copolymerization promoted by [Pd(Me)(MeCN)(*m*-Bz-BIOX)][X] (X = OTf, BF_4, PF_6) in CH_2Cl_2/MeOH (9:1): syndiotactic copolymers with a different degree of stereoregularity are obtained, and the highest stereoregularity has been reported for the polyketone prepared with the triflate derivative.[21] The triflate induces the highest degree of stereoregularity even in the CO/*p*-Me-styrene copolymerization promoted by [Pd(η^1,η^2-C_8H_{12}OMe)(N′-N′)][X] (N′-N′ = (2,6-Me_2Ph)-N=C(Me)-C(Me)=N-(2,6-Me_2Ph); X = OTf, PF_6, BArF) in CH_2Cl_2.[22]

Herein we have found that: 1) changing the solvent from CH_2Cl_2 to trifluoroethanol results in a decrease in the stereochemical control, but the copolymer is still isotactic; 2) in trifluoroethanol the catalyst with triflate leads to the copolymer with the lowest stereochemical control.

In conclusion, analysis of the overall results indicates that in dichloromethane the best stereochemical control is obtained by catalysts with the most strongly coordinating anion, while in trifluoroethanol the catalyst with the most strongly coordinating anion exerts the least control on the stereochemistry.

To elucidate the reactions involved in the initiation and termination steps of the catalytic cycle, the end-group characterization of the polyketones synthesized in trifluoroethanol, with precatalysts **1a**, **2** and **3**, was performed by MALDI-TOF analysis. No difference is observed in the three spectra. They are characterized by several series of peaks, for five of which a structural identification can be proposed. They correspond to six different polymeric chains, a, b, c, d, e, and f, cationized with Na^+. The macromolecules differ from the end-groups, while the repetitive unit (132 Da) is that expected for this kind of copolymerization reaction (Figure 5). Two chains have a trifluorocarboalkoxy end-group and both of them terminate with an organic fragment involving hydroquinone (chains a and b in Figure 6).

Two other chains initiate with a saturated group and differ from the termination, which is the unsaturated group or the hydroxy fragment (chains c and d in Figure 6). Chains b and c give rise to a series of peaks whose differences in mass are too low to distinguish them with the instrumental set-up employed. Chain e is characterized by carboxylic acid and trifluorocarboalkoxy fragments as end-groups (Figure 6). Even though the different clusters in the spectra are separated by the mass of the usual CO/styrene repetitive unit, the key feature of this chain is the presence of an addi-

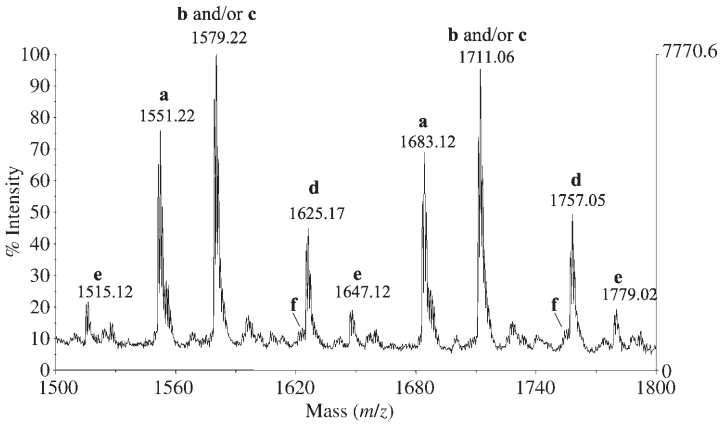

Figure 5. MALDI-TOF mass spectra of the CO/styrene polyketone synthesized in TFE with precatalyst **1a**.

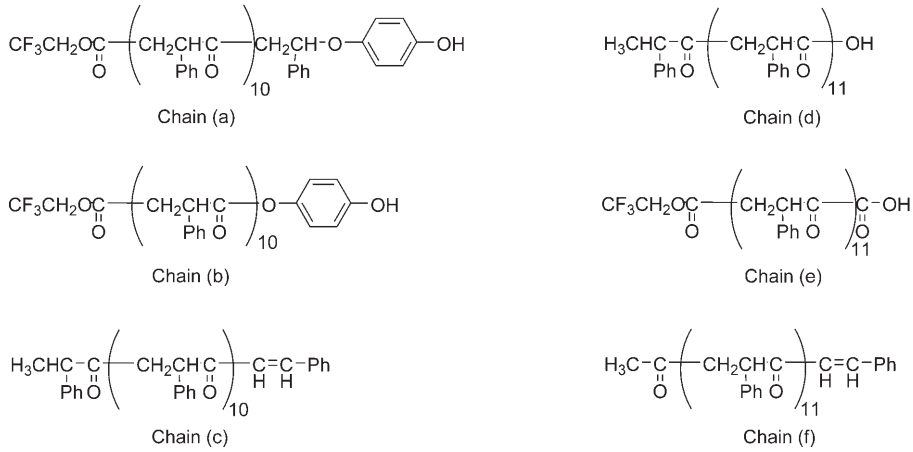

Figure 6. Polymeric chains present in the CO/styrene polyketones.

tional carbonyl group resulting from a double carbonylation reaction followed by chain termination,[24] yielding an unexpected end-group. Chain f features a ketonic and an unsaturated end-group (Figure 6).

The present MALDI-TOF analysis depicts a more complicated scenario than that observed when the bischelated complexes with phenanthroline ligands are used as precatalysts.[9b] The activation step consists in migratory insertion of the Pd–Me group on the coordinated carbon monoxide, followed by propagation of the polymeric chain, which is terminated by the β-hydrogen elimination reaction yielding chain f and the Pd–H intermediate. The Pd–hydride species is the key intermediate for this reaction and represents the central core of four different catalytic cycles (Scheme 1).

Our previous investigations on the copolymerization mechanism operative in trifluoroethanol, in the absence of benzoquinone, indicated that the fluorinated alcohol does not give rise to termination through alcoholysis and that β-hydrogen elimination is the unique chain transfer process. These data were also corroborated by a detailed study on the alcoholysis reaction taking place on Pd–acyl species with a series of different alcohols.[25] Therefore, the triflurocarboalkoxy group of chains a, b, and e represents the initiation of the chain, which derives from the oxidation of the Pd–H intermediate by the 1,4-benzoquinone, which is concomitantly reduced to hydroquinone. This is a typical process taking place when the copolymerization is carried out in an alcoholic medium in the presence of the oxidant.[9a,26] Chains a and b terminate with an organic fragment, which is the result of the nucleophilic attack of one of the two alcoholic functions of 1,4-hydroquinone on the growing chain. In contrast to the usual methanolysis, which occurs on the Pd–C(acyl) bond only, the alcoholysis involving the 1,4-hydroquinone takes place on both the Pd–C(acyl) and the Pd–C(alkyl) bonds, yielding an ester end-group (chain b in Figure 6) and an ether end-group (chain a in Figure 6), respectively. The formation of the aryl-ether might occur with a mechanism analogous to that proposed in the literature for the catalytic synthesis of diaryl ethers promoted by palladium complexes.[27]

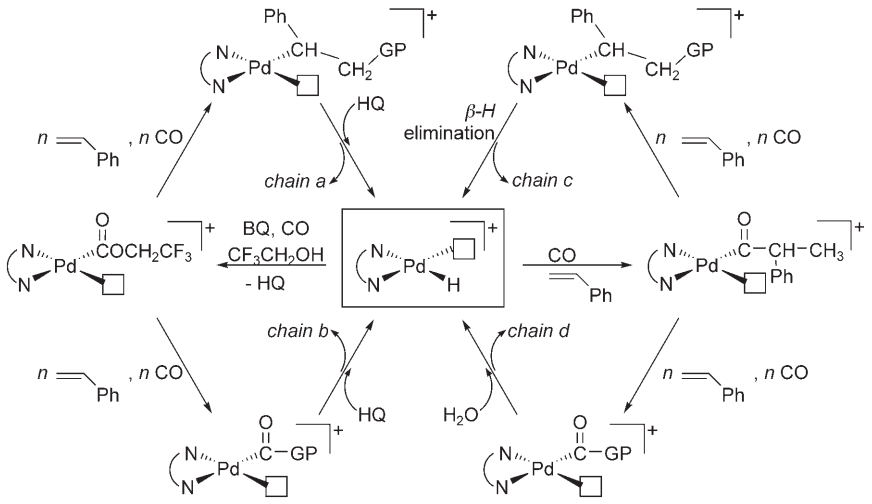

Scheme 1. The proposed catalytic cycles. GP = growing polymer.

Even though the effect of 1,4-hydroquinone, and not of 1,4-benzoquinone, as a regulator of the molecular weight of the polymeric chains was reported some years ago,[28] it has never been found present as an end-group of the polymeric chains. Moreover, some carbonylation experiments on styrene in methanol, in the presence of a low concentration of hydroquinone, led to the formation of methyl *p*-hydroxyphenyl 2-phenylbutanedioate, thus indicating that alcoholysis of acyl intermediates by phenols is more rapid than that by alcohols.[28a] Not only are the results reported here in perfect agreement with this previous study, but they also demonstrate the capability of 1,4-hydroquinone to give alcoholysis on the Pd–C(alkyl) bond, thus doubling the probability of an alcoholysis chain transfer process. The role of hydroquinone makes it possible to explain the decrease in molecular weight observed both on increasing the benzoquinone concentration and on prolonging the reaction time (Table 5).

The palladium species resulting from attack by 1,4-hydroquinone on the polymeric chain should be the Pd–H derivative, which can either reenter the trifluorocarboalkoxy pathways or insert one molecule of styrene to start chains c or d (Figure 6, Scheme 1). The termination reactions of these chains could be the β-hydrogen elimination (chain c, Figure 6), or the attack of water yielding a carboxylic acid end-group (chain d, Figure 6). The palladium species resulting from these termination reactions is always the hydride derivative.

Conclusion

The chemistry of (*S,S*)-*i*Pr-BIOX ligand coordination to palladium has been studied. Both mononuclear and dinuclear species are isolated, depending on the nature of the anion. The latter complexes represent one of the first examples of bridging coordination mode for this ligand. The ^{1}H NMR investigation provided evidence that the protons of the isopropyl substituents and protons in position 4 of the hydroxazole rings can be regarded as "probe protons" to identify the coordination mode of the BIOX ligand: their chemical shifts differ depending on whether the ligand is bridging two palladium ions or whether it is chelated to one metal center only.

It was already known that complex **3** catalyzes the synthesis of the isotactic CO/styrene copolymer.[5a] We have now shown that the catalyst performance can be enhanced by one order of magnitude by carrying out the copolymerization in trifluoroethanol. At the same time, however, changing the reaction medium caused a partial loss of the stereochemical control during the polymerization process. Moreover, in the fluorinated alcohol the effect of the anion on the copolymer stereochemistry was also evident. The origin of the observed effects on the polymer tacticity is still unclear and it is under current investigation.

The MALDI-TOF analysis of the synthesized polyketones indicated the major role played by the hydroquinone in this catalytic system.

The importance of trifluoroethanol in ensuring the stability of the Pd–hydride species has been confirmed definitively.

Experimental Section

General procedures: $[Pd(OAc)_2]$ was a loan from Engelhard Italia and was used as received. The nitrogen-donor ligand, (*S,S*)-*i*Pr-BIOX,[29] and NaBArF[30] were prepared according to published procedures. 2,2,2-Trifluoroethanol (Aldrich) and the analytical grade solvents (Fluka) were used without further purification for synthetic, spectroscopic, and catalytic purposes. The dichloromethane used for the synthesis of complexes and for the catalytic tests was purified by distillation over $CaCl_2$, and stored under an inert atmosphere. Carbon monoxide (CP grade, 99.9%) was supplied by SIAD. ES-MS spectra were obtained on a Perkin-Elmer AP1; samples were dissolved in CH_2Cl_2. ^{1}H NMR spectra were recorded at 400 MHz on a JEOL EX400; the resonances were referenced to the solvent peak versus TMS ($CDCl_3$ at $\delta = 7.26$ ppm and CD_2Cl_2 at $\delta = 5.33$ ppm). ^{13}C NMR spectra of polyketones were recorded at 125 MHz on a Bruker AMX 500 MHz at the Eidgenössische Technische Hochschule, Zürich.

Syntheses: The manipulations were carried out under an argon atmosphere by standard Schlenk techniques, at room temperature, following the procedures reported in the literature.[10,12] *trans*-$[Pd(Cl)_2(PhCN)_2]$[31] and [Pd(Cl)(Me)(cod)][32] were synthesized following the procedures reported in the literature.

Synthesis of $[Pd(CH_3)(Cl)((S,S)$-*i*Pr-BIOX)] (4) and $[Pd(CH_3)(Cl)(\mu$-(S,S)-*i*Pr-BIOX)]$_2$ (4a): (*S,S*)-*i*Pr-BIOX (0.23 g, 1.04 mmol) was added to a stirred solution of [Pd(Cl)(CH_3)(cod)] (cod = 1,5-cyclooctadiene) (0.25 g, 0.94 mmol) in CH_2Cl_2 (15 mL). After the mixture had been stirred for 1 h at room temperature in the dark, the solution was filtered over Celite, washed with CH_2Cl_2, and concentrated to half its original volume under vacuum. Upon addition of diethyl ether, an orange oil was obtained. After treatment in liquid nitrogen it became a yellow solid, which was filtered under vacuum and washed with hexane. Crystals of **4** suitable for X-ray structure determination were obtained directly from the synthesis. Recrystallization from dichloromethane/hexane afforded crystals of both **4** and **4a** suitable for X-ray analysis.

4: Yield: 0.33 g, 92%. ^{1}H NMR (400 MHz, $CDCl_3$, 25°C): δ = 0.84–0.94 (m, 12H, CH(CH_3)$_2$), 1.02 (s, 3H, Pd–CH_3), 2.26 (m, 1H, CH(CH$_3$)$_2$), 2.74 (m, 1H, CH(CH$_3$)$_2$), 4.26 (m, 1H, H^4), 4.37 (m, 1H, H$^{4'}$), 4.53 (m, 2H, H^5), 4.74 ppm (m, 2H, H$^{5'}$); elemental analysis calcd (%) for $C_{13}H_{23}ClN_2O_2Pd$: C 40.96, H 6.08, N 7.35; found: C 41.7, H 6.17, N 7.32.

4a: ^{1}H NMR (400 MHz, $CDCl_3$, 25°C): δ = 0.99 (s, 3H, Pd–CH_3), 0.84–1.19 (m, 12H, CH(CH_3)$_2$), 2.48 (m, 1H, CH(CH$_3$)$_2$), 2.78 (m, 1H, CH-(CH$_3$)$_2$), 4.29 (m, 1H, H^4), 4.37–4.74 (m, 2H, H^5 and H$^{5'}$), 5.10 ppm (m, 1H, H$^{4'}$); elemental analysis calcd (%) for $C_{26}H_{46}Cl_2N_4O_4Pd_2$: C 40.96, H 6.08, N 7.35; found: C 41.4, H 6.26, N 7.25.

Synthesis of $[Pd(CH_3)(OTf)(\mu$-(S,S)-*i*Pr-BIOX)]$_2$ (1a): A solution of AgOTf (0.113 g, 0.44 mmol) in anhydrous acetonitrile was added to a stirred suspension of **4** (0.152 g, 0.40 mmol) in CH_2Cl_2 (10 mL). After 30 min the solution was filtered to remove the silver salts, and concentrated under vacuum. Addition of diethyl ether caused the precipitation of a yellow solid, which was filtered off, washed with diethyl ether, and dried under vacuum. From the mother liquor it was possible to isolate crystals for X-ray structure determination.

Yield: 0.18 g, 93%. ^{1}H NMR (400 MHz, CD_2Cl_2, 25°C): δ = 1.08 (br, 24H, CH(CH_3)$_2$), 1.14 (s, 6H, Pd-CH_3), 2.57 (br, 2H, CH(CH$_3$)$_2$), 2.71 (br, 2H, CH(CH$_3$)$_2$), 4.30 (m, 2H, H^4), 4.42–4.64 (m, 4H, H^5 and H$^{5'}$), 4.82 ppm (m, 2H, H$^{4'}$); ^{19}F NMR (188.29 MHz, CD_2Cl_2): δ = −78.7 ppm; MS (60 eV): *m/z* (%): 991 (37) $[M]^+$, 975 (10) $[M-CH_3]^+$, 842 (27) $[M-OTf]^+$, 737 (100) $[M-2CH_3-i$Pr-BIOX$]^+$, 331 (15) $[M-2CH_3-i$Pr-BIOX$-2OTf]^+$; elemental analysis calcd (%) for $C_{28}H_{46}F_6N_4O_{10}Pd_2S_2$: C 33.98, H 4.68, N 5.66; found: C 32.0, H 3.73, N 5.52.

Synthesis of [Pd(CH$_3$)(CH$_3$CN)-((*S,S*)-*i*Pr-BIOX)][PF$_6$] (2): A solution of $AgPF_6$ (0.111 g, 0.44 mmol) in anhydrous acetonitrile was added to a stirred suspension of **4** (0.152 g, 0.40 mmol) in CH_2Cl_2 (10 mL). After 30 min the solution was filtered to remove the silver salt and concentrated under vacuum. Addition of diethyl ether caused the formation of a brown oil, which was transformed into a yellow solid upon treatment in liquid nitrogen. The solid was filtered off, washed with diethyl ether, and dried under vacuum.

Yield: 70%. ^{1}H NMR (400 MHz, CD_2Cl_2, 25°C): δ = 0.83–1.08 (m, 12H, CH(CH_3)$_2$), 1.10 (s, 3H, Pd–CH$_3$), 2.02–2.13 (m, CH(CH$_3$)$_2$), 2.24 (br, CH(CH$_3$)$_2$), 2.33 (s, CH_3CN), 2.38 (s, CH_3CN), 2.60 (m, CH(CH$_3$)$_2$), 4.22 and 4.31 (m, 1H, H^4 or H$^{4'}$) 4.51–4.80 ppm (m, 5H, H^4 or H$^{4'}$ and H^5, H$^{5'}$); MS (60 eV): *m*/*z* (%): 676 (100) [2*M*−CH$_3$−2CH$_3$CN]$^{3+}$, 660 (70) [2*M*−2CH$_3$−2CH$_3$CN]$^{4+}$, 389 (20) [*M*]$^+$, 375 (26) [*M*−CH$_3$CN]$^+$; elemental analysis calcd (%) for $C_{15}H_{26}F_6N_3O_2PPd$: C 33.88, H 4.93, N 7.90; found: C 32.9, H 5.14, N 7.13.

Table 7. Crystallographic data and details of structure refinements of compounds **1a**, **4**, and **4a**.

	1a	**4**	**4a**·0.5 CH$_2$Cl$_2$
formula	$C_{28}H_{46}F_6N_4O_{10}Pd_2S_2$	$C_{13}H_{23}ClN_2O_2Pd$	$C_{26.5}H_{47}Cl_3N_4O_4Pd_2$
M_r	989.61	381.18	804.83
crystal system	orthorhombic	orthorhombic	triclinic
space group	$P2_12_12_1$	$P2_12_12_1$	$P1$
a [Å]	10.418(3)	8.380(3)	11.679(3)
b [Å]	16.731(4)	9.969(4)	11.569(4)
c [Å]	22.981(4)	20.045(4)	16.123(4)
α [°]			97.17(2)
β [°]			97.81(3)
γ [°]			119.67(3)
volume [Å^3]	4005.7(17)	1674.6(10)	1827.9(9)
Z	4	4	2
ρ_{calcd} [g cm^{-3}]	1.641	1.512	1.462
$\mu Mo_{K\alpha}$ [mm^{-1}]	1.083	1.267	1.236
F(000)	2000	776	818
θ_{max} [°]	26.73	29.93	27.48
reflns collected	42839	16792	14805
unique reflections	8486	4351	14805
R_{int}	0.0310	0.0286	–
observed $I>2\sigma(I)$	6765	3986	10037
parameters	475	176	710
goodness of fit (F^2)	1.038	1.178	0.980
R_1 ($I>2\sigma(I)$)[a]	0.0459	0.0449	0.0526
wR_2[a]	0.1150	0.1038	0.1319
residuals [e Å^{-3}]	0.548, −0.435	1.570, −0.741	0.711, −0.829

[a] $R_1 = \Sigma||F_o|-|F_c||/\Sigma|F_o|$, $wR_2 = [\Sigma w(F_o^2-F_c^2)^2/\Sigma w(F_o^2)^2]^{1/2}$.

Synthesis of [Pd(CH$_3$)(CH$_3$CN)-((*S,S*)-*i*Pr-BIOX)][BArF] (3): A solution of NaBArF (0.26 g, 0.30 mmol) in anhydrous CH_3CN was added to a stirred suspension of **4** (0.10 g, 0.26 mmol) in CH_2Cl_2 (8 mL). After 1 h the solution was filtered over Celite and concentrated under vacuum. Addition of diethyl ether caused the precipitation of a brown oil, which was transformed into a red solid upon treatment in liquid nitrogen. The solid was filtered off, washed with diethyl ether, and dried under vacuum.

Yield: 0.30 g, 92%. ^{1}H NMR (400 MHz, CD_2Cl_2, 25°C): δ = 0.83–1.00 (m, 12H, CH(CH_3)$_2$), 1.11 (s, 3H, Pd–CH$_3$), 2.01 (m, 1H, CH(CH$_3$)$_2$), 2.12 (m, 1H, CH(CH$_3$)$_2$), 2.34 (s, 3H, CH$_3$CN), 4.22 (m, 2H, H^4 and H$^{4'}$), 4.59–4.83 (m, 4H, H^5 and H$^{5'}$), 7.73 (br, 4H, aromatics), 7.73 ppm (m, 8H, aromatics); MS (60 eV): *m*/*z* (%): 386 (100) [*M*]$^+$, 372 (10) [*M*−CH$_3$]$^+$, 345 (24) [*M*−CH$_3$CN]$^+$, 331 (90) [*M*−CH$_3$−CH$_3$CN]$^+$; elemental analysis calcd (%) for $C_{47}H_{38}BF_{24}N_3O_2Pd$: C 45.16, H 3.06, N 3.36; found: C 44.3, H 2.92, N 3.49.

NMR experiments in situ: CD_2Cl_2 (0.70 mL) was added to an NMR tube (5 mm) charged with the complex (7.5×10^{-3} mmol). When needed, 2,2,2-trifluoroethanol (2.7 μL) was added. CO was then bubbled for 5 min through a needle inserted through a rubber cap into the NMR tube. The ^{1}H NMR spectrum was obtained after 15 min.

X-ray crystal structure determination of 1a, 4, and 4a: Diffraction data for the structures reported were determined at room temperature (293(2) K) on a Nonius DIP-1030H system with $Mo_{K\alpha}$ radiation (λ = 0.71073 Å). A total of 30 frames were collected, each with an exposure time of 15–20 min, a rotation angle of 6° about ϕ, and the detector at 80–90 mm from the crystal. Cell refinement, indexing, and scaling of the data sets were carried out using Mosflm and Scala[33] for **1a** and **4** and Denzo[34] for **4a**. All the structures were solved by direct methods and Fourier analyses[35] and refined by the full-matrix least-squares method based on F^2 with all the observed reflections.[35] A difference Fourier map of (**4a**) shows two disordered molecules of dichloromethane (each with 0.5 occupancy). All the calculations were performed using the WinGX System, Version 1.64.05.[36] Crystal data and details of refinements are reported in Table 7.

CCDC-263342–CCDC-263344 contain the supplementary crystallographic data for this paper. These data can be obtained free of charge from the Cambridge Crystallographic Data Centre via www.ccdc.cam.ac.uk/data_request/cif.

Copolymerization: Copolymerization reactions were carried out in a thermostated glass reactor equipped with a magnetic stirrer under a CO atmosphere. After introduction of the catalyst precursor, the benzoquinone, the solvent (20 mL), and styrene (10 mL), carbon monoxide was bubbled for 10 min into the reaction mixture heated at 30°C. The system was then closed and connected to a balloon containing CO. After the appropriate reaction time, the reaction mixture was poured into methanol (100 mL). The polymer was filtered off, washed with methanol, and dried under vacuum.

Molecular weight measurements: The molecular weights $\langle M_w\rangle$ of copolymers and the molecular weight distributions ($\langle M_w\rangle/\langle M_n\rangle$) were determined by gel-permeation chromatography versus polystyrene standards. The analyses were recorded on a Knauer HPLC (K-501 Pump, K-2501 UV-detector) with a PLgel 5 μm×10^4 Å GPC column and chloroform as solvent (flow rate 0.6 mL min^{-1}). To dissolve the copolymer, the sample (3 mg) was solubilized with 1,1,1,3,3,3-hexafluoro-2-propanol (120 μL) and chloroform was added up to 10 mL. The statistical calculations were performed by using the Bruker Chromstar software program.

MALDI/MS measurements: MALDI mass measurements were performed on a Voyager-DE PRO instrument (Applied Biosystems, Foster City, CA, USA), operating in reflectron positive-ion mode. Ions formed by a pulsed UV laser beam (λ = 337 nm) were accelerated at 20 keV. The instrumental conditions were: mirror ratio 1.12; grid voltage 77%; guide wire 0.05%; delay time 150 ns. (2-(*p*-Hydroxyphenylazo)benzoic acid (HABA) was used as a matrix (10 mg mL^{-1} in $CHCl_3$). Copolymer (2 mg) was dissolved in $CHCl_3$ (1 mL) and a portion (5 μL) of this solution was added to the same volume of the matrix solution. About 1 μL of the resulting solution was deposited on the stainless steel sample holder and allowed to dry before introduction into the mass spectrometer. Three independent measurements were made for each sample.

External mass calibration was done using the Calibration Mixture 1 of the Sequazyme Peptide Mass Standards Kit, based on the monoisotopic values of [*M*+H]$^+$ of des-Arg^1-bradykinin, angiotensin I, Glu^1-fibrino-

peptide B and neurotensin at *m*/*z* 904.4681, 1296.6858, 1570.6774, and 1672.9175, respectively.

Acknowledgements

This work was supported by the Ministero dell'Istruzione, dell'Università e della Ricerca (MIUR—Rome; PRIN No. 2003033857 and PRIN No. 2003039774) and by the European Network "Palladium" (Fifth Framework Program, contract No. HPRN-CT-2002–00196). Engelhard Italia is gratefully acknowledged for a generous loan of $[Pd(OAc)_2]$.

[1] a) G. W. Coates, P. D. Hustad, S. Reinartz, *Angew. Chem.* **2002**, *114*, 2340–2361; *Angew. Chem. Int. Ed.* **2002**, *41*, 2236–2257; b) J. Tiang, G. W. Coates, *Angew. Chem.* **2000**, *112*, 3772–3775; *Angew. Chem. Int. Ed.* **2000**, *39*, 3626–3629.

[2] Y. Okamoto, T. Nakano, *Chem. Rev.* **1994**, *94*, 349–372.

[3] K. Nozaki, in *Catalytic Synthesis of Alkene–Carbon Monoxide Copolymers and Cooligomers* (Ed.: A. Sen), Kluwer Academic Publishers, Dordrecht, **2003**, pp. 217–235.

[4] a) M. Brookhart, M. I. Wagner, A. A. Balavoine, H. A. Haddou, *J. Am. Chem. Soc.* **1994**, *116*, 3641–3642; b) M. Brookhart, M. I. Wagner, *J. Am. Chem. Soc.* **1996**, *118*, 7219–7220.

[5] a) S. Bartolini, C. Carfagna, A. Musco, *Macromol. Rapid Commun.* **1995**, *16*, 9–14; b) B. Binotti, C. Carfagna, G. Gatti, D. Martini, L. Mosca, C. Pettinari, *Organometallics* **2003**, *22*, 1115–1123.

[6] a) G. Consiglio, B. Milani, in *Catalytic Synthesis of Alkene–Carbon Monoxide Copolymers and Cooligomers* (Ed.: A. Sen), Kluwer Academic Publishers, Dordrecht, **2003**, pp. 189–215; b) M. T. Reetz, G. Haderlein, K. Angermund, *J. Am. Chem. Soc.* **2000**, *122*, 996–999; c) A. Bastero, C. Claver, A. Ruiz, S. Castillón, E. Daura, C. Bo, E. Zangrando, *Chem. Eur. J.* **2004**, *10*, 3747–3760.

[7] K. Nozaki, N. Sato, H. Takaya, *J. Am. Chem. Soc.* **1995**, *117*, 9911–9912.

[8] a) M. Sperrle, A. Aeby, G. Consiglio, A. Pfaltz, *Helv. Chim. Acta* **1996**, *79*, 1387–1392; b) A. Aeby, G. Consiglio, *Inorg. Chim. Acta* **1999**, *296*, 45–51.

[9] a) B. Milani, A. Anzilutti, L. Vicentini, A. Sessanta o Santi, E. Zangrando, S. Geremia, G. Mestroni, *Organometallics* **1997**, *16*, 5064–5075; b) B. Milani, G. Corso, G. Mestroni, C. Carfagna, M. Formica, R. Seraglia, *Organometallics* **2000**, *19*, 3435–3441; c) B. Milani, A. Scarel, G. Mestroni, S. Gladiali, R. Taras, C. Carfagna, L. Mosca, *Organometallics* **2002**, *21*, 1323–1325; d) A. Scarel, B. Milani, E. Zangrando, M. Stener, S. Furlan, G. Fronzoni, G. Mestroni, S. Gladiali, C. Carfagna, L. Mosca, *Organometallics* **2004**, *23*, 5593–5605.

[10] A. Scarel, J. Durand, D. Franchi, E. Zangrando, G. Mestroni, B. Milani, S. Gladiali, C. Carfagna, B. Binotti, S. Bronco, T. Gragnoli, *J. Organomet. Chem.* **2005**, *690*, 2106–2120.

[11] H. A. McManus, P. J. Guiry, *Chem. Rev.* **2004**, *104*, 4151–4202, and references therein.

[12] B. Milani, A. Marson, E. Zangrando, G. Mestroni, J. M. Ernesting, C. J. Elsevier, *Inorg. Chim. Acta* **2002**, *327*, 188–201.

[13] A. Bastero, A. Ruiz, C. Claver, B. Milani, E. Zangrando, *Organometallics* **2002**, *21*, 5820–5829.

[14] a) G. K. Patra, I. Goldberg, S. K. Chowdhury, B. C. Maiti, A. Sarkar, P. R. Bangal, S. Chakravorti, N. Chattopadhyay, D. A. Tocher, M. G. B. Drew, G. Mostafa, S. Chowdhury, D. Datta, *New J. Chem.* **2001**, *25*, 1371–1373; b) G. K. Patra, I. Goldberg, A. Sarkar, S. Chowdhury, D. Datta, *Inorg. Chim. Acta* **2003**, *344*, 7–14.

[15] a) D. M. Haddleton, D. J. Duncalf, A. J. Clark, M. C. Crossman, D. Kukulj, *New J. Chem.* **1998**, *22*, 315–317; b) R. E. Marsh, A. L. Spek, *Acta Crystallogr. Sect. B* **2001**, *57*, 800–805.

[16] A. K. El-Qisairi, H. A. Qaseer, P. M. Henry, *J. Organomet. Chem.* **2002**, *656*, 168–176.

[17] a) G. Baum, E. C. Constable, D. Fenske, C. E. Housecroft, T. Kulke, M. Neuburger, M. Zehnder, *J. Chem. Soc. Dalton Trans.* **2000**, 945–959; b) G. Baum, E. C. Constable, D. Fenske, C. E. Housecroft, T. Kulke, *Chem. Eur. J.* **1999**, *5*, 1862–1873; c) V. Amendola, L. Fabbrizzi, C. Mangano, P. Pallavicini, E. Roboli, M. Zema, *Inorg. Chem.* **2000**, *39*, 5803–5806; d) H. Mürner, A. von Zelewsky, G. Hopfgartner, *Inorg. Chim. Acta* **1998**, *271*, 36–39; e) O. Mamula, A. von Zelewsky, G. Bernardinelli, *Angew. Chem.* **1998**, *110*, 302–305; *Angew. Chem. Int. Ed.* **1998**, *37*, 289–293.

[18] A. Macchioni, G. Bellachioma, G. Cardaci, M. Travaglia, C. Zuccaccia, B. Milani, G. Corso, E. Zangrando, G. Mestroni, C. Carfagna, M. Formica, *Organometallics* **1999**, *18*, 3061–3069.

[19] A. Gsponer, Dissertation No. 14698, ETH, Zurich.

[20] A. Gsponer, B. Milani, G. Consiglio, *Helv. Chim. Acta* **2002**, *85*, 4074–4078.

[21] D. Sirbu, G. Consiglio, B. Milani, P. G. A. Kumar, P. S. Pregosin, S. Gischig, *J. Organomet. Chem.* **2005**, *690*, 2254–2262.

[22] B. Binotti, C. Carfagna, C. Zuccaccia, A. Macchioni, *Chem. Commun.* **2005**, 92–93.

[23] M.-C. Chen, J. A. S. Roberts, T. J. Marks, *J. Am. Chem. Soc.* **2004**, *126*, 4605–4625, and references therein.

[24] a) J.-T. Chen, A. Sen, *J. Am. Chem. Soc.* **1984**, *106*, 1506–1507; b) M. Sperrle, G. Consiglio, *J. Organomet. Chem.* **1996**, *506*, 177–180.

[25] P. W. N. M. van Leeuwen, M. A. Zuideveld, B. H. G. Swennenhuis, Z. Freixa, P. C. J. Kamer, K. Goubitz, J. Fraanje, M. Lutz, A. L. Spek, *J. Am. Chem. Soc.* **2003**, *125*, 5523–5539.

[26] E. Drent, P. H. M. Budzelaar, *Chem. Rev.* **1996**, *96*, 663–681.

[27] a) G. Mann, C. Incarvito, A. L. Rheingold, J. F. Hartwig, *J. Am. Chem. Soc.* **1999**, *121*, 3224–3225; b) A. Aranyos, D. W. Old, A. Kiyomori, J. P. Wolfe, J. P. Sadighi, S. L. Buchwald, *J. Am. Chem. Soc.* **1999**, *121*, 4369–4378.

[28] a) C. Pisano, S. C. A. Nefkens, G. Consiglio, *Organometallics* **1992**, *11*, 1975–1978; b) M. Barsacchi, G. Consiglio, L. Medici, G. Petrucci, U. W. Suter, *Angew. Chem.* **1991**, *103*, 992–994; *Angew. Chem. Int. Ed. Engl.* **1991**, *30*, 989–991.

[29] S. E. Denmark, R. A. Stavenger, A.-M. Faucher, J. P. Edwards, *J. Org. Chem.* **1997**, *62*, 3375–3389.

[30] M. Brookhart, B. Grant, A. F. Volpe Jr, *Organometallics* **1992**, *11*, 3920–3922.

[31] L. Chatt, L. M. Vallarino, L. M. Venanzi, *J. Chem. Soc.* **1957**, 3413–3416.

[32] R. E. Rülke, J. M. Ernesting, A. L. Spek, C. J. Elsevier, P. W. N. M. van Leeuwen, K. Vrieze, *Inorg. Chem.* **1993**, *32*, 5769–5778.

[33] Collaborative Computational Project, Number 4 , *Acta Crystallogr. Sect. D* **1994**, *50*, 760–763.

[34] Z. Otwinowski, W. Minor, Processing of X-ray diffraction data collected in oscillation mode, in: *Methods in Enzymology*, *Vol. 276*: *Macromolecular Crystallography, Part A* (Eds.: C. W. Carter Jr., R. M. Sweet), Academic Press, New York, **1997**, pp. 307–326.

[35] G. M. Sheldrick, SHELX97 Programs for Crystal Structure Analysis (Release 97-2). University of Göttingen, Germany, **1998**.

[36] L. J. Farrugia, *J. Appl. Crystallogr.* **1999**, *32*, 837–838.

Received: April 12, 2005
Published online: July 27, 2005

